THE JOURNAL OF IMMUNOLOGY

Coordinated Control of Immunity to Muscle Stage *Trichinella spiralis* by IL-10, Regulatory T Cells, and TGF- β

Daniel P. Beiting, Lucille F. Gagliardo, Matthias Hesse, Susan K. Bliss, Diana Meskill and Judith A. Appleton

J Immunol 2007; 178:1039-1047; ;
doi: 10.4049/jimmunol.178.2.1039
http://www.jimmunol.org/content/178/2/1039

The Journal of Immunology is published twice each month by
The American Association of Immunologists, Inc.,
9650 Rockville Pike, Bethesda, MD 20814-3994.

Print ISSN: 0022-1767 Online ISSN: 1550-6606.

Coordinated Control of Immunity to Muscle Stage *Trichinella spiralis* by IL-10, Regulatory T Cells, and TGF-β[1]

Daniel P. Beiting,* Lucille F. Gagliardo,* Matthias Hesse,† Susan K. Bliss,* Diana Meskill,* and Judith A. Appleton[2†]

We previously demonstrated that IL-10 is critical in the control of acute inflammation during development of *Trichinella spiralis* in the muscle. In this study, we use gene-targeted knockout mice, adoptive transfer of specific T cell populations, and in vivo Ab treatments to determine the mechanisms by which inflammation is controlled and effector T cell responses are moderated during muscle infection. We report that $CD4^+CD25^-$ effector T cells, rather than $CD4^+CD25^+$ regulatory T cells, suppress inflammation by an IL-10-dependent mechanism that limits IFN-γ production and local inducible NO synthase induction. Conversely, we show that depletion of regulatory T cells during infection results in exaggerated Th2 responses. Finally, we provide evidence that, in the absence of IL-10, TGF-β participates in control of local inflammation in infected muscle and promotes parasite survival. *The Journal of Immunology,* 2007, 178: 1039–1047.

Trichinella spiralis is a natural pathogen of rodents that establishes chronic infection in skeletal muscle and is well suited for the study of helminth-induced immune suppression. During a relatively brief intestinal phase, adult female worms release newborn larvae (NBL)[3] that rapidly enter mesenteric venules (1), disseminate throughout the host, and eventually enter skeletal muscle. The diaphragm, tongue, and masseter muscles are all preferred sites of infection in mice (2). Each NBL invades a single, terminally differentiated muscle cell (myotube) and, over a period of 20 days, both the parasite and the host cell undergo a process of coordinated growth and development, marked by dramatic host cell remodeling (3–6). If larvae survive this developmental period, they establish a chronic infection that is essential for transmission. To investigate the mechanisms that control T cell responses specifically to muscle stage *T. spiralis*, we synchronously infected mice with NBL delivered i.v. Using this route of infection, we can evaluate the immune response to muscle larvae without the confounding influences of intestinal adult worm survival and fecundity.

Chronic helminth infections are often associated with polarized Th2 responses and the production of the anti-inflammatory cytokines IL-10 and TGF-β (7–9). It is unclear which cell types serve as critical sources of IL-10 to regulate inflammation and limit T cell responses in vivo. Moreover, there is a paucity of studies that have addressed the importance of IL-10/TGF-β cooperation in vivo during infection. Understanding the specific cell types required for IL-10-mediated suppression during helminth infection and the additional cytokine signals important for this process will help to elucidate the mechanisms of long-term T cell modulation.

Naturally occurring regulatory T cells (Treg), defined by the surface expression of CD4 and the IL-2R α-chain (CD25) and intracellular expression of the transcription factor forkhead box P3 (Foxp3), regulate Th1-driven intestinal inflammation through mechanisms that require IL-10 and TGF-β (10, 11). In recent years, these suppressive cells have been implicated as potential regulators of helminth-induced responses, but the nature of Treg-mediated suppression and the role of IL-10 in this process remain controversial. For example, in mice immunized with eggs from the human helminth parasite *Schistosoma mansoni*, the Treg cell population expands in parallel with effector T cells (Teff) and limits both Th1 and Th2 responses in an IL-10-independent manner (12, 13). In contrast, earlier studies conducted in *S. mansoni*-infected mice showed that both $CD4^+CD25^+$ Treg and $CD4^+CD25^-$ Teff isolated from liver granulomas produced IL-10 in response to egg Ags (14, 15) and suppressed egg-specific IFN-γ production after adoptive transfer into $IL\text{-}10^{-/-}$ mice (15). Conversely, when Treg were depleted in mice infected with the filarial parasite *Litomosoides sigmodontis*, production of the Th2 cytokines IL-4 and IL-5, as well as IL-10, were increased (16). These varying results underscore the importance of examining Treg-mediated suppression during other helminth infections to more completely understand the mechanisms by which regulation of effector function is achieved.

In addition to limiting inflammation, tight regulation of Teff responses can promote parasite persistence. It is clear that TH2 responses are protective against intestine-dwelling helminth parasites (17). IL-4 and IL-13 promote mastocytosis (18), smooth muscle hypercontractility (19), goblet cell hyperplasia, and mucus secretion that are critical to the timely expulsion of nematodes from the gut (20–22). In the absence of IL-10, the intestinal nematode *Trichuris muris* induces more pronounced Th1 responses, thereby limiting Th2-driven expulsion, prolonging infection and causing increased mortality (23). Helminth parasites often have tissue migratory phases and occupy more than one anatomical niche during the life cycle, yet little is known about what constitutes a protective response against parenteral stages of helminths where the pathogen

*James A. Baker Institute for Animal Health and †Department of Microbiology and Immunology, College of Veterinary Medicine, Cornell University, Ithaca, NY 14853

Received for publication August 14, 2006. Accepted for publication November 9, 2006.

The costs of publication of this article were defrayed in part by the payment of page charges. This article must therefore be hereby marked *advertisement* in accordance with 18 U.S.C. Section 1734 solely to indicate this fact.

[1] This research was supported by a grant to J.A.A. from the National Institutes of Health (A114490). D.P.B. was supported by Training Grant T32-AI07643.

[2] Address correspondence and reprint requests to Dr. Judith A. Appleton, James A. Baker Institute for Animal Health, College of Veterinary Medicine, Cornell University, Ithaca, NY 14853. E-mail address: jaa2@cornell.edu

[3] Abbreviations used in this paper: NBL, newborn larvae; Treg, regulatory T cell; Foxp3, forkhead box P3; Teff, effector T cell; KO, knockout; CLN, cervical lymph node; dpi, days postinjection; WT, wild type; iNOS, inducible NO synthase; 1°/2°, primary/secondary.

must often be destroyed rather than simply displaced from its habitat. Although the *S. mansoni* granuloma has been invaluable in understanding how IL-10 limits tissue pathology (24), egg deposition in the liver is not essential to the completion of the *S. mansoni* life cycle, making it difficult to link the control of immunity with survival and transmission of the parasite.

In this study, we use gene-targeted knockout (KO) mice, adoptive transfer of specific T cell populations, and in vivo Ab treatments to determine the mechanisms by which inflammation is controlled and Teff responses are regulated during muscle infection with *T. spiralis*. The results reveal a cooperative interplay among IL-10, TGF-β, Teff, and Treg that ensures parasite survival while protecting the host from inflammatory disease.

Materials and Methods

Rats and mice

Adult Albino Oxford strain rats were produced and maintained in the James A. Baker Institute Vivarium. C57BL/10$^{SgSnAi-(ko)IL10}$ (IL-10$^{-/-}$) and C57BL/10$^{SgSnAi-(ko)IL10-(ko)RAG2}$ (RAG2$^{-/-}$ × IL-10$^{-/-}$) were bred at the Cornell Transgenic Mouse Core Facility and maintained at the James A. Baker Institute. Six-week-old C.129S2-STAT6^{tm1Gru}/J (STAT6$^{-/-}$) mice were obtained from The Jackson Laboratory. Age- and gender-matched C57BL/10^{SgSnAiTac} and BALB/c^{AnNTac} mice were obtained from Taconic Farms. RAG2$^{-/-}$ × IL-10$^{-/-}$ were maintained in a Bioclean isolation unit (Lab Products). Mice and rats were fed autoclaved, pelleted ration (5K67; The Jackson Laboratory), and acidified water (pH 3). Animal care was in accordance with the guidelines of the American Association for Accreditation of Laboratory Animal Care and experiments were performed with the approval of the Institutional Animal Care and Use Committee of Cornell University.

Parasite

T. spiralis (pig strain) infectious larvae (L_1) were recovered from muscles of irradiated Albino Oxford rats by digestion with 1% pepsin in acidified water as described by Crum et al. (25). Newborn larvae were recovered from adult worm cultures prepared as described previously (26). Mice were administered a single injection into the lateral tail vein of 25,000 NBL suspended in 0.25 ml of serum-free DMEM (Mediatech). Infection by this route bypasses the intestinal phase of infection, eliminating the intestinal immune response as a confounding variable. In addition, injection of NBL results in synchronous development of nurse cells and the host response to muscle infection. Typically, we find that approximately one-half of the NBL injected establish chronic infection (data not shown). In other experiments, mice were injected with 5,000 NBL, rested for 3 mo, and then challenged i.v. with 20,000 NBL. Mice were euthanized by CO_2 inhalation at the times indicated in each experiment. Muscle larvae burdens were determined as described previously (26). To evaluate infectivity of parasites that developed in experimental mice, muscle larvae recovered from individual mice were pooled and C57BL/10 mice were infected with 250 L_1. At ~30 days after oral infection, muscle burdens were determined to confirm that larvae from different treatment groups were equally infective. Somatic Ags from mature muscle larvae were prepared from whole larval homogenate as described previously (27).

Antibodies

Rat mAb to the IL-2R α-chain (CD25; IgG1, clone PC61 (28)); mouse mAb to TGF-β (IgG1, clone 1D11 (29); American Type Culture Collection); and mouse mAb to equine influenza virus (IgG1, clone 5 (30)) were affinity purified from culture supernatant using protein G and fast performance liquid chromatography (Akta FPLC; Amersham Biosciences). The column was equilibrated with 0.02 M sodium phosphate (pH 7.0), and bound protein was eluted with 0.1 M glycine-HCl (pH 2.7). Fractions were neutralized with 1 M Tris-HCl (pH 9.0). Purified Ab was dialyzed against PBS. Total rat Ig was precipitated from normal sera with 40% ammonium sulfate (Sigma-Aldrich) and dialyzed as described above. After endotoxin removal over polymyxin B columns (Detoxi-Gel; Pierce), all Ab preparations contained <1.0 unit endotoxin/mg as determined using the *Limulus* amebocyte lysate pyrochrome assay (Associates of Cape Cod).

For flow cytometry experiments, FITC-conjugated anti-CD4 (clone GK1.5, 1 μg/ml; eBioscience), allophycocyanin-conjugated anti-Foxp3 (clone FJK-16s, 5 μg/ml), biotinylated anti-CD25 (clone 7D4; recognizes an epitope distinct from that bound by clone PC61, 1 μg/ml; BD Pharmingen), and streptavidin-PE (1 μg/ml; eBioscience) were used. For immunohistochemistry, rabbit polyclonal Ab raised against the C terminus of mouse inducible NO synthase (iNOS, 0.34 μg/ml; Lab Vision) was detected with biotinylated goat anti-rabbit Ig (1 μg/ml; Vector Laboratories). Negative control sections were treated with either biotinylated mouse anti-llama IgG1 (31) or normal rabbit serum.

Histology and immunohistochemistry

Histochemical staining was conducted as described previously (26). For immunohistochemistry, formalin-fixed, paraffin-embedded sections were mounted on poly-L-lysine-coated glass slides, deparaffinized for 10 min in xylene, and rehydrated through graded alcohol baths. Ag retrieval was conducted by steaming tissue sections in a rice steamer (Black & Decker) for 40 min in 10 mM citric acid (pH 6.0). Sections were allowed to cool for 20 min at room temperature. Staining was conducted as described previously (26). Slides were dehydrated through graded alcohol baths, cleared in xylene, and mounted in Permount (Fisher Scientific).

Recovery and culture of lymphocytes from cervical lymph nodes (CLN)

CLN drain the tongue and masseter muscles in the mouse and were used to monitor the immune response to muscle infection. CLN were excised from infected mice and kept on ice in DMEM supplemented with 10% FCS (Atlanta Biologicals), 0.1 M nonessential amino acids (Invitrogen Life Technologies), 30 mM HEPES (Invitrogen Life Technologies), and 50 μM 2-ME (Sigma-Aldrich). CLN from individual mice were manually dispersed, under aseptic conditions, in petri dishes using a 12-ml syringe pestle. Cells were passed through sterile 100-μm screens, washed with medium, and cell number was determined using a Coulter Counter (model Z2; Beckman Coulter). Cells were plated in triplicate at 1×10^6 cells/well in 200 μl on 96-well tissue culture plates (Costar, Corning) and stimulated with 10 μg/well somatic larval Ag to elicit cytokine secretion from parasite-specific T cells. Additional triplicate wells were cultured either in the absence of Ag (medium only) or in the presence of plate-bound anti-CD3 (no azide, low endotoxin; clone 145-2C11, BD Pharmingen) as a pan-T cell stimulus. Cells were incubated in 8% CO_2 and supernatants were collected after 72 h and stored at −20°C.

Cytokine-specific ELISA

ELISA to measure concentrations of IL-4, IL-5, IL-10 and IFN-γ was conducted as described previously (32). IL-13 ELISA used capture (clone 38321, 2 μg/ml) and detecting Abs (goat polyclonal, 0.1 μg/ml) from R&D Systems. The sensitivities of the assays were 100 pg/ml (IL-5, 10, 13 and IFN-γ) or 20 pg/ml (IL-4).

Flow cytometry

Cells were recovered from individual diaphragms by digestion in collagenase I and stained for flow cytometric analysis as described previously (26).

Adoptive transfer experiments

Single-cell suspensions were prepared from CLN recovered from wild-type (WT; $n = 8$) and IL-10$^{-/-}$ ($n = 8$) donor mice at 20 days postinjection (dpi) as described above. CD4$^+$CD25$^+$ and CD4$^+$CD25$^-$ cells were purified from CLN using the Mouse Regulatory T Cell Isolation kit (Miltenyi Biotec) and an AutoMACS magnetic cell separator. CLN cells were subjected to two rounds of negative selection for CD4$^+$ T cells and were 97% pure in flow cytometric analysis (data not shown). CD25$^+$ Treg and CD25$^-$ Teff populations were then enriched by positive and negative selection. Treg carried 6% CD4$^+$CD25$^-$ cells and Teff cells carried 3% CD4$^+$CD25$^+$ cells. RAG2$^{-/-}$/IL10$^{-/-}$ mice received 1×10^4 CD4$^+$CD25$^+$ cells and 1×10^5 CD4$^+$CD25$^-$ cells i.p. Mice were i.v. infected with 25,000 NBL the following day. At 13 dpi, CLN cells and tongue were collected for cytokine assays and histochemistry, respectively.

In vivo Ab treatments

For depletion of CD25$^+$ cells, mice were injected once i.p. with 750 μg of anti-CD25 or rat Ig (control). The following day, mice were injected with 25,000 NBL. At 20 dpi, cells were recovered from diaphragm and stained for flow cytometric analysis to confirm extent of Treg depletion. In separate experiments, mice were administered 1 mg of neutralizing Ab to TGF-β or mouse anti-influenza (control) each week beginning on day −1. Mice were infected on day 0 and sera collected at 20 dpi were assayed for active TGF-β.

Luminescence-based TGF-β bioassay

Active TGF-β was assayed in sera as described previously (16) using mink lung epithelial cells (clone 32, provided by Dr. D. Rifkin, New York University Medical Center, New York, NY) cultured in X-VIVO-15 serum-free medium (Cambrex). Luminescence was measured using the luminescent substrate system (Promega) and a Veritas Microplate Luminometer equipped with reagent injectors (Turner). The concentration of active or total TGF-β in sera was determined using a standard curve prepared with recombinant human TGF-β1 (Roche Diagnostic Systems).

Statistical analysis

Each experiment was conducted two or three times. Means and SDs were calculated from data collected from individual mice. Significance was determined using a Student's *t* test or one-way ANOVA with Tukey's post hoc analysis. Statistical analysis was performed with GraphPad Prism 4 software.

Results

Influence of IL-10 on the development of the T cell response to muscle infection

We previously demonstrated that IL-10 limits inflammation during parasite development in the muscle, but does not contribute to immune modulation during chronic infection (26). To better define the influence of IL-10 on the cellular response to muscle infection, we examined the cytokine secretion profile of CLN cells recovered from WT and IL-10$^{-/-}$ mice during parasite development (8 dpi; acute muscle infection) and at the completion of parasite development (21 dpi; transition to chronic infection). After stimulation with somatic larval Ags, WT CLN cells produced IL-10 and IFN-γ (Fig. 1*A*) at 8 dpi. At 21 dpi, IL-10 production was increased, IL-5 and IL-13 production was detectable, and IFN-γ production was unchanged (Fig. 1*B*). In the absence of IL-10, cells produced nearly eight times more IFN-γ at 8 dpi (Fig. 1*C*) and 21 dpi (Fig. 1*D*), compared with WT counterparts. In contrast, Th2 cytokine production was not significantly influenced by IL-10 deficiency. Parallel cultures stimulated with anti-CD3 yielded similar cytokine profiles, although the magnitude of the responses was greater than that obtained with specific Ag stimulation (data not shown). We did not detect significant levels of IL-4, IL-5, IL-10, IL-13, or IFN-γ in uninfected WT or IL-10$^{-/-}$ mice after stimulation with somatic Ag (data not shown).

IFN-γ is a potent activator of macrophage activity, stimulating production of iNOS and enhanced generation of reactive oxygen intermediates. We have shown previously that the cellular infiltrate recruited to infected muscle is rich in macrophages. Sections of infected tongue were stained with Ab to iNOS to determine whether the increase in IFN-γ observed in IL-10$^{-/-}$ mice would translate to enhanced macrophage activation in vivo. Nurse cells in WT mice rarely had iNOS^{+} cells at 21 dpi (Fig. 1*E*). In contrast, iNOS-producing cells were abundant near infected myotubes of IL-10$^{-/-}$ mice (Fig. 1*F*). These data suggest that IL-10 limits inflammation during parasite development by suppressing IFN-γ levels and limiting local iNOS production, but does not influence the development of a Th2 response later in infection.

Influence of Th2 cytokines on the inflammatory response to muscle infection

To further investigate the influence of Th2 cytokines during muscle infection, we infected mice that were deficient in STAT6. These mice are on a BALB/c background. BALB/c mice would be expected to mount a stronger Th2 response than the C57BL/10 mice used in previous experiments. STAT6 is required to transduce signals from IL-4 and IL-13 bound to surface receptors (33). STAT6$^{-/-}$ ($n = 6$) or BALB/c ($n = 5$) control mice were synchronously infected. Tongues recovered from BALB/c mice at 18 dpi contained numerous mature larvae and fully developed nurse cells surrounded by focal infiltrates (Fig. 2*A*). In contrast, nurse cells of STAT6$^{-/-}$ mice had markedly reduced inflammatory infiltrates around infected cells (Fig. 2*B*) and reduced numbers of CLN cells (Fig. 2*D*). When cultured in the presence of somatic larval Ags, CLN cells from BALB/c mice at 18 dpi produced significantly more IL-4, IL-5, and IL-13, but less IFN-γ, compared with their STAT6$^{-/-}$ counterparts (Fig. 2*C*). IL-10 concentrations were comparable in BALB/c and STAT6$^{-/-}$ mice. These results support the conclusion that even in the absence of Th2 cytokines, IL-10 controls the proinflammatory effects of a Th1 response. In other experiments, we infected IL-10/4 double KO mice and observed a phenotype similar to that of IL-10$^{-/-}$ mice (data not shown), confirming that IL-10 controls the proinflammatory effects of a Th1 response. Finally, despite impairment of Th2 responses and inflammation in STAT6$^{-/-}$ mice, larval burdens were similar to those in BALB/c mice (Fig. 2*E*). Larvae recovered from BALB/c and STAT6$^{-/-}$ mice were equally infective for normal mice, producing muscle burdens of 25,867 ± 6,275 L_1 ($n = 3$) and 17,133 ± 4,868 L_1 ($n = 3$), respectively.

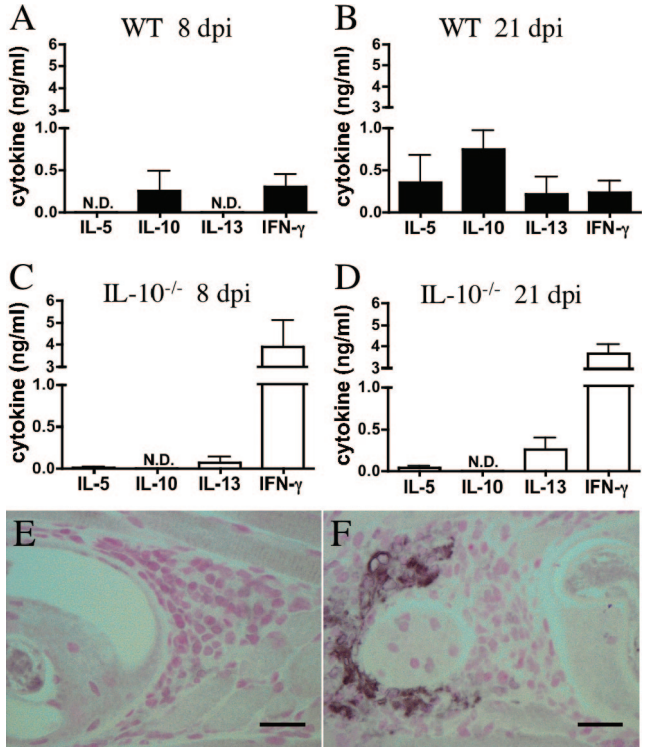

FIGURE 1. The influence of IL-10 on development of the T cell response to muscle infection. *A–D*, Cytokines produced by CLN collected from C57BL/10 (WT) mice and IL-10$^{-/-}$ mice at 8 and 21 dpi. Cells were stimulated with somatic larval Ag. Means and SDs are shown from groups of three to five mice. N.D., Not detected. *E* and *F*, Immunohistochemical detection of iNOS at 21 dpi in WT (*E*) and IL-10$^{-/-}$ (*F*) mice. iNOS-producing cells are brown. Scale bars, 25 μm.

Depletion of naturally occurring Treg during muscle infection

Treg can suppress Th1-driven intestinal inflammation through mechanisms that require IL-10 (10, 11). To determine whether naturally occurring Treg were required for the IL-10-dependent suppression of IFN-γ during muscle infection, C57BL/10 mice were injected with Ab to CD25 (clone PC61). This treatment has been reported to deplete Treg; however, recent evidence suggests that anti-CD25 functionally inactivates Treg by inducing the down-regulation of the IL-2 receptor (34). To determine the extent of Treg depletion/inactivation, we recovered cells that infiltrated

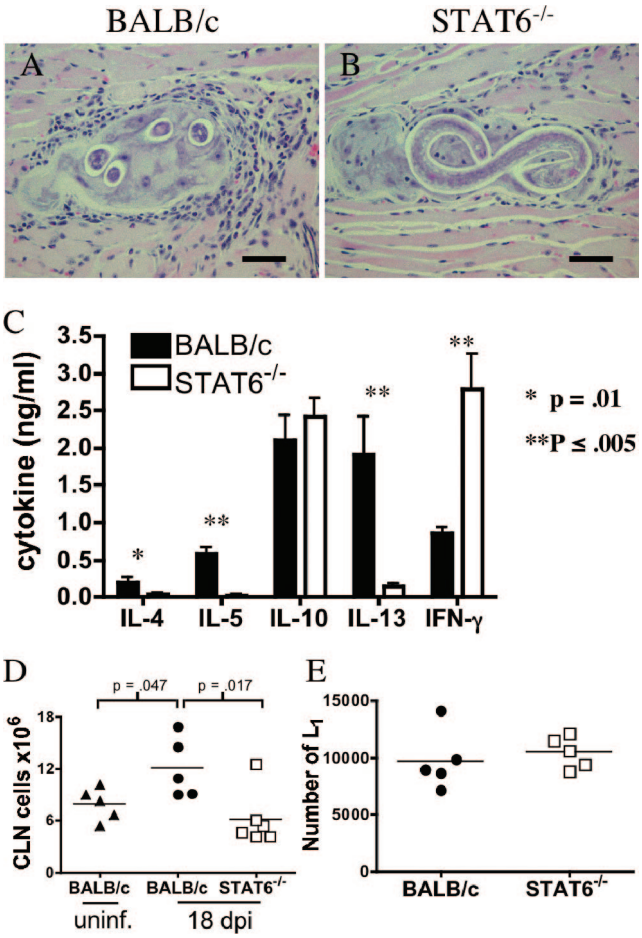

FIGURE 2. The influence of STAT6 signaling on the inflammatory response to muscle infection. *A* and *B*, H&E-stained tissue sections of tongues from BALB/c (*A*) and STAT6$^{-/-}$ (*B*) mice at 18 dpi. *C*, Cytokines produced after somatic Ag stimulation of CLN cells from STAT6$^{-/-}$ (n = 6) and BALB/c mice (n = 5). *D*, CLN cell numbers, 18 dpi. *E*, Larval burdens, 18 dpi. Symbols in *D* and *E* represent individual mice. Scale bars, 50 μm. Significance was determined by Student's t test.

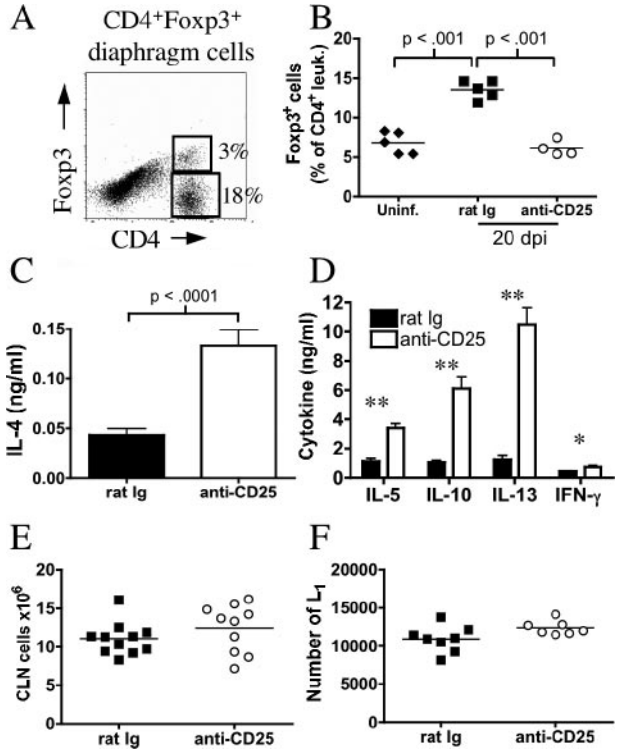

FIGURE 3. Depletion of naturally occurring Treg during muscle infection. *A*, Representative dot plot of diaphragm cells showing CD4$^+$ and CD4$^+$Foxp3$^+$ cells as a percentage of gated lymphocytes at 20 dpi. *B*, Foxp3$^+$ cells as a percentage of CD4$^+$ cells from uninfected and 20 dpi diaphragm from rat Ig-treated and anti-CD25-treated mice. *C* and *D*, IL-4, IL-5, IL-10, IL-13, and IFN-γ produced after Ag-specific stimulation of CLN cells from mice treated with anti-CD25 (n = 10) or rat Ig (n = 11). *E*, CLN cell numbers, 20 dpi. *F*, Larval burden in muscles, 20 dpi. Significance was determined by one-way ANOVA with Tukey's post hoc analysis (*B*) or Student's t test (*C* and *D*); ∗, p = 0.016 and ∗∗, $p < 0.001$. Symbols in *B*, *E*, and *F* represent individual mice.

the diaphragms of Treg-depleted or control mice at 20 dpi. Cells were stained with Abs to CD4, CD25, and Foxp3 for analysis by flow cytometry. We found that 8.4 ± 1.5% of diaphragm leukocytes expressed CD25 at 20 dpi. Treatment with anti-CD25 reduced this percentage to 4.6 ± 1.0% ($p < 0.01$). In addition to being expressed on the surfaces of Treg, CD25 is also transiently up-regulated on the surfaces of Teff after activation (35, 36). To confirm that anti-CD25 treatment depleted Treg, we analyzed the proportion of diaphragm CD4$^+$ cells that expressed Foxp3 at 20 dpi. Staining of diaphragm cells with anti-CD4 and anti-Foxp3 yielded a distinct CD4$^+$Foxp3$^+$ cell population (Fig. 3*A*). In diaphragms of uninfected mice, ~7% of the CD4$^+$ cells expressed Foxp3 (Fig. 3*B*). This percentage increased to ~14% at 20 dpi and was reduced by one-half by in vivo treatment with anti-CD25 (Fig. 3*B*). Reduction of Foxp3$^+$ cells correlated with dramatically elevated production of IL-4, IL-5, IL-10, and IL-13 by CLN cells stimulated with parasite Ag (Fig. 3, *C* and *D*). A modest but significant increase in IFN-γ was also detected. Despite exaggerated Th2 responses, cellularity in CLN and larval burdens were unchanged (Fig. 3, *E* and *F*). Larvae recovered from Treg-depleted and control mice at 20 dpi were equally infective when passaged into WT mice, producing muscle burdens of 40,250 ± 8,826 L_1 (n = 4) and 38,333 ± 6,691 L_1 (n = 3), respectively. These data show that naturally occurring Treg accumulate in infected muscle. Reducing this population of cells by in vivo Ab treatment led to a significant increase in Th2 cytokine responses but did not alter the numbers of CLN cells. In these ways, the results of Treg depletion were dramatically different from IL-10 deficiency.

Teff-derived IL-10 is sufficient to suppress local inflammation and IFN-γ production during muscle infection

To determine the cell type responsible for IL-10-mediated suppression of local inflammation during infection, we established an adoptive transfer system in which we could limit the source of IL-10 to donor-derived Treg or Teff. Enriched Treg and Teff populations were prepared from CLN recovered from WT and IL-10$^{-/-}$ mice at 20 dpi. A total of 1 × 10^4 Treg was transferred along with 1 × 10^5 Teff, a ratio that is normally found in mice (37). Recipient RAG2$^{-/-}$/IL10$^{-/-}$ mice are deficient in T and B lymphocytes and have no endogenous source of IL-10. Thus, transferred Treg or Teff were the only source of IL-10. Mice that received WT Teff were able to control myositis, regardless of whether these cells were transferred along with WT (Fig. 4*A*) or IL-10$^{-/-}$ Treg (Fig. 4*B*). In contrast, mice receiving IL-10$^{-/-}$ Teff, whether in combination with WT (Fig. 4*C*) or IL-10$^{-/-}$ Treg (Fig. 4*D*), had more extensive myositis. Ag-induced IFN-γ production (Fig. 4*E*) and local iNOS synthesis (data not shown) were observed only in mice that received Teff from IL-10$^{-/-}$ donors, irrespective of the source of Treg. These findings suggests that

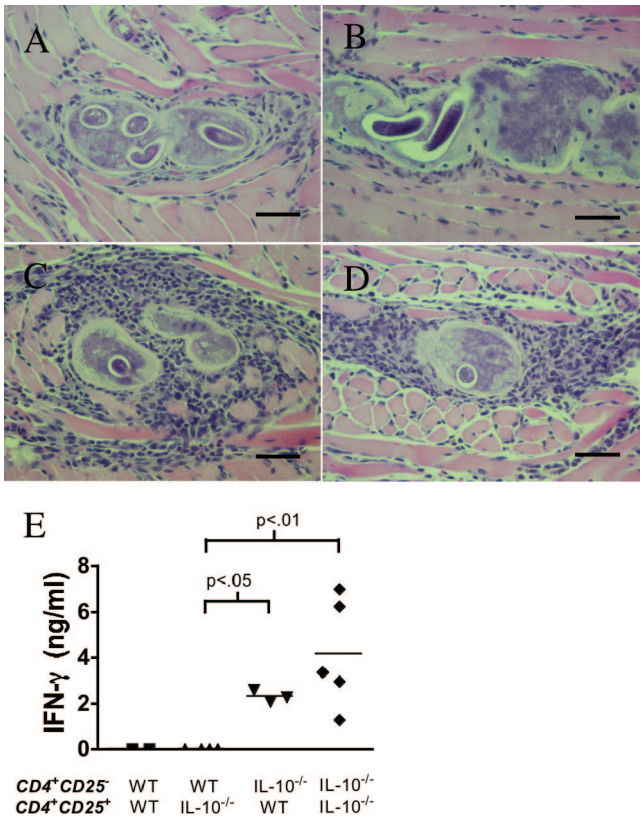

FIGURE 4. Contributions of $CD4^+CD25^-$ and $CD4^+CD25^+$ cells to IL-10-mediated suppression of inflammation in infected muscle. *A–D*, H&E-stained sections of diaphragm from $RAG2^{-/-}$/$IL\text{-}10^{-/-}$ mice at 13 dpi that received the following: *A*, $CD4^+CD25^-$ and $CD4^+CD25^+$ cells from WT donor mice; *B*, WT $CD4^+CD25^-$ cells and $IL\text{-}10^{-/-}$ $CD4^+CD25^+$ cells; *C*, $IL\text{-}10^{-/-}$ $CD4^+CD25^-$ cells and WT $CD4^+CD25^+$ cells; or *D*, $CD4^+CD25^-$ and $CD4^+CD25^+$ cells from $IL\text{-}10^{-/-}$ donors. *E*, IFN-γ produced by CLN cells from recipient mice after stimulation with somatic Ags. Symbols represent individual mice. Significance was determined by one-way ANOVA with Tukey's post hoc analysis. Scale bars, 50 μm.

IL-10 produced by $CD4^+CD25^-$ cells is sufficient to suppress myositis and IFN-γ.

Effect of TGF-β neutralization on the cytokine and inflammatory response to muscle infection

Both surface-bound and secreted TGF-β have been shown to be important mechanisms of Treg-mediated control of Teff (38–40). To evaluate a role for TGF-β in control of myositis, we neutralized this cytokine in vivo by weekly administration of a mAb (clone 1D11) that neutralizes activity of TGF-β1 and β2 isoforms (29). We determined the extent of neutralization using a bioassay that measures the active form of TGF-β (41). Muscle infection with *T. spiralis* induced a significant elevation of active TGF-β in sera of $IL\text{-}10^{-/-}$ but not WT mice (Fig. 5*A*). Treatment with TGF-β-neutralizing Ab reduced circulating levels of the active cytokine to preinfection levels (Fig. 5*A*). CLN from WT mice treated with anti-TGF-β produced significantly more IL-13 and less IFN-γ compared with control Ig-treated WT mice (Fig. 5*B*). In contrast, neutralization of TGF-β in $IL\text{-}10^{-/-}$ mice caused a reduction in IL-13 production (Fig. 5*C*).

As expected, WT mice treated with control Ig had limited myositis at 20 dpi, whereas $IL\text{-}10^{-/-}$ mice treated with control Ig had larger infiltrates surrounding nurse cells (Fig. 5, *D* and *F*). Cellular infiltration was moderate in WT mice treated with anti-TGF-β

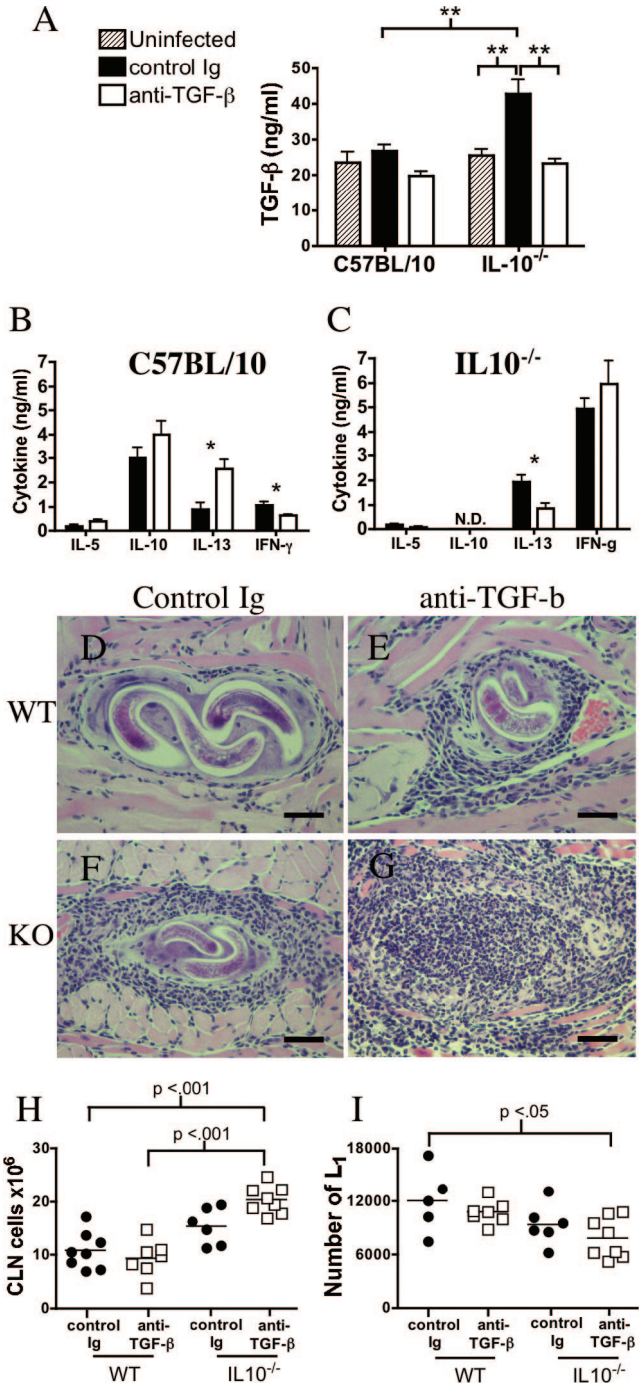

FIGURE 5. Influence of TGF-β on muscle infection in WT and $IL\text{-}10^{-/-}$ mice. *A*, Active TGF-β in sera of uninfected ($n = 5$) and 20 dpi WT and $IL10^{-/-}$ mice. *B* and *C*, Cytokines produced after somatic Ag stimulation of CLN cells from WT mice treated with anti-TGF-β ($n = 7$) or control Ig ($n = 8$) (*B*), or $IL\text{-}10^{-/-}$ mice treated with anti-TGF-β ($n = 8$) or control Ig ($n = 6$) (*C*). N.D., Not detected. ∗, $p < 0.05$ and ∗∗, $p < 0.001$ as determined by Student's *t* test. *D–G*, H&E-stained tongue sections collected at 20 dpi from WT and $IL\text{-}10^{-/-}$ (KO) mice treated with control Ig or anti-TGF-β. *H*, CLN cell numbers, 20 dpi. *I*, Larval burdens in muscles, 20 dpi. Scale bars, 50 μm. Symbols represent individual mice in *H* and *I*. Significance was determined by one-way ANOVA and Tukey's post hoc test.

(Fig. 5*E*). Mice deficient in IL-10 and treated with anti-TGF-β had the most extensive cellular infiltration of muscle (Fig. 5*G*) and the most cellular CLN (Fig. 5*H*). Although IL-10 or TGF-β alone did not significantly protect muscle larvae from destruction, the combined

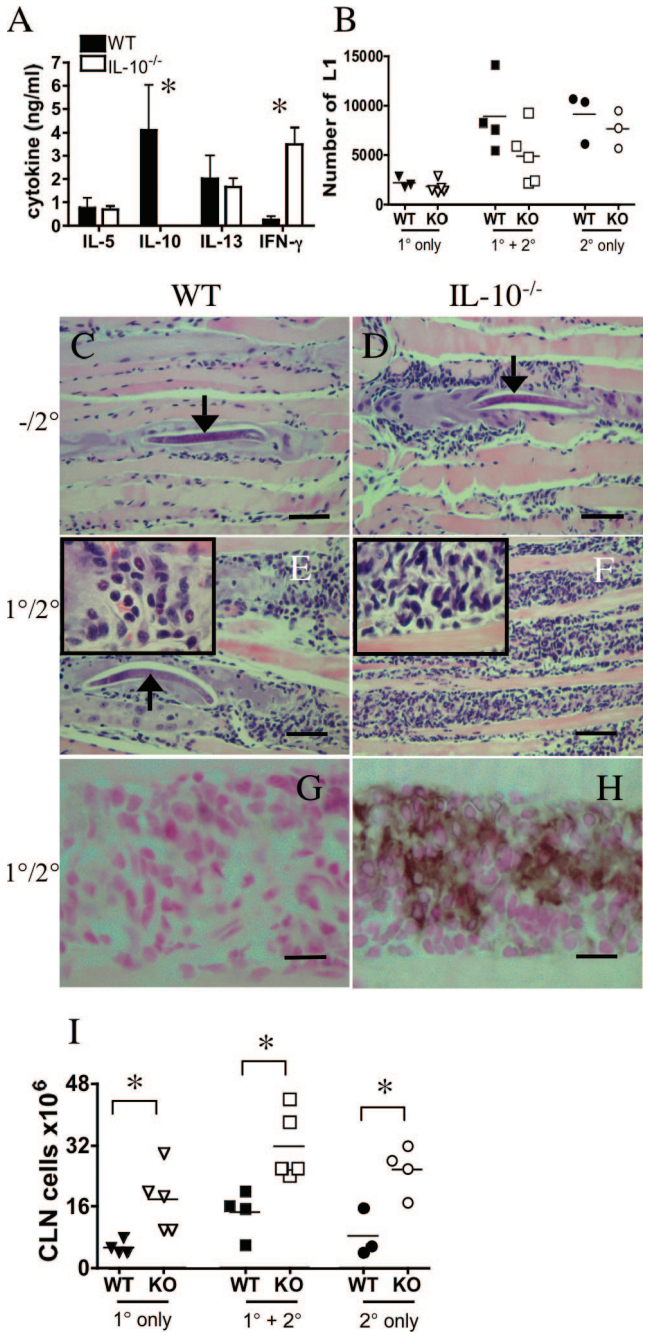

FIGURE 6. Response to NBL challenge. *A*, Cytokines produced after somatic Ag stimulation of CLN cells recovered from WT and IL-$10^{-/-}$ mice 8 days postchallenge. *B*, Larval burdens in muscles, 21 dpi. *C–F*, H&E-stained sections of tongue from C57BL/10 (WT) and IL-$10^{-/-}$ mice receiving prime and challenge (1°/2°) or only the secondary infection (−/2°). *G* and *H*, Immunohistochemical detection of iNOS in sections of diaphragm from WT (*G*) and IL-$10^{-/-}$ (*H*) mice. *I*, CLN cell numbers, 8 dpi. Arrows, Immature larvae. Scale bars, 50 μm. Symbols represent individual mice in *B* and *I*. ∗, $p \leq 0.023$ as determined by Student's *t* test.

deficiency in both cytokines resulted in a significant reduction in muscle larvae burden compared with WT mice treated with control Ig (Fig. 5*I*). Viable larvae recovered from all four groups of mice were equally infective when passaged into normal mice ($n = 5$ for each group) producing muscle burdens of 15,200 ± 4,361 L_1 (WT, control Ig); 23,600 ± 4,347 L_1 (WT, anti-TGF-β); 25,880 ± 11,140 L_1 (IL-$10^{-/-}$, control Ig); and 16,240 ± 6,121 L_1 (IL-$10^{-/-}$, anti-TGF-β).

Effects of Th2-polarized or mixed Th1/Th2 responses on survival of muscle stage parasites

We reasoned that T cell responses capable of destroying larvae would serve as logical targets of suppression during infection. To better understand the type of immune response that is required for destruction of muscle larvae, we developed an in vivo challenge model in which WT and IL-$10^{-/-}$ mice were first infected with a low dose of parasites (5,000 NBL), rested for 3 mo to allow the larvae to establish a chronic infection, and then challenged with 20,000 NBL to elicit a memory response (primary/secondary (1°/2°)). For controls, additional mice received either the priming dose only (1°/−), or the challenge dose only (−/2°). WT mice receiving both priming and challenge infections mounted a polarized Th2 response characterized by IL-5, IL-10, and IL-13 production, with little IFN-γ (Fig. 6*A*). In contrast, cells from IL-$10^{-/-}$ mice produced significantly more IFN-γ, but similar quantities of IL-5 and IL-13, compared with WT mice (Fig. 6*A*). If larvae survived the Th2-polarized response to challenge infection in WT mice, we would expect 1°/2° mice to harbor the combined burdens of the 1° infection (2,221 ± 575 L_1) and the 2° infection (9,066 ± 2,505 L_1) to give an expected burden of ~11,287 L_1, yet 1°/2° WT mice had a mean muscle burden of only 8,874 L_1 ± 3,679 at 20 days postchallenge (Fig. 6*B*). If larvae survived the mixed response to challenge in IL-$10^{-/-}$ mice, we would expect 1°/2° mice yield worm burdens of ~9,432 L_1, rather than the observed mean burden of 4,915 ± 2,878 (48% killing; Fig. 6*B*).

Although the worm burdens in the challenge groups were not reduced sufficiently to achieve statistical significance, killing of larvae was evident in histological sections of the diaphragm. WT mice receiving only the secondary infection had no cellular infiltrate surrounding developing larvae at 8 dpi (Fig. 6*C*). In contrast, WT 1°/2° mice had extensive infiltrates in muscle (Fig. 6*E*), characterized by a cellular infiltrate rich in eosinophils (Fig. 6*E*, *inset*). Compared with WT mice, IL-$10^{-/-}$ mice receiving only a secondary infection had more intense inflammatory reactions surrounding developing larvae (Fig. 6*D*). The most severe myositis was seen in IL-$10^{-/-}$ 1°/2° mice (Fig. 6*F*), in which an infiltrate largely comprised of mononuclear cells and nearly devoid of eosinophils (Fig. 6*F*, *inset*) incarcerated some larvae. Entry of large numbers of inflammatory cells into the nurse cell occurs during nurse cell destruction and parasite death. Large numbers of iNOS-producing cells were detected in the diaphragms of primed and challenged IL-$10^{-/-}$ (Fig. 6*H*) but not WT mice (Fig. 6*G*). Significant increases in CLN size occurred along with increased myositis, with 1°/2° IL-$10^{-/-}$ mice having the most cellular CLN (Fig. 6*I*). Thus, the exaggerated local Th1 response was associated with larval killing.

Discussion

Our previous work demonstrated a role for IL-10 in limiting inflammation during *T. spiralis* development in the muscle, yet the cell types responsible for this modulation, as well as the mechanism by which IL-10 effected suppression, were not identified. The data presented here show that IL-10 limits acute inflammation, suppresses IFN-γ levels, and prevents iNOS production by inflammatory cells recruited to the site of infection. In our system, IL-10 deficiency does not influence the production of IL-4, IL-5, or IL-13 during muscle infection, nor does it impair the generation of parasite-specific IgG1 (26), suggesting that IL-10-producing cells specifically suppress Th1 responses during muscle infection. Our results contrast with findings reported from *S. mansoni*-infected

mice, where IL-10 limits not only IFN-γ production, but also production of the Th2 cytokines IL-4 and IL-5 (42, 43). This difference in the targets of regulation may relate to the different habitats occupied by the two organisms. Although *S. mansoni* eggs are extracellular in liver and gut, larval *T. spiralis* are intracellular in muscle. The suppression of Th1 responses by IL-10 during *T. spiralis* infection may reflect a biological adaptation to limit intracellular killing mechanisms during larval development within muscle cells.

Our data are compatible with a role for IFN-γ in promoting inflammation observed in IL-$10^{-/-}$ mice but do not eliminate possible influences of other proinflammatory mediators (e.g., TNF-α). In a murine model of Th1-driven intestinal inflammation, neutralization of IFN-γ in IL-$10^{-/-}$ animals was effective in preventing colitis if given early, but did not ameliorate established disease if administered later (44, 45), suggesting that IFN-γ drives inflammation, but may not sustain it. IL-10 also preferentially limits Th1 responses induced by filarial nematodes (46). Th1 stimuli have been investigated in filarial nematodes, and it has been reported that surface Ags of the endosymbiotic bacterium *Wolbachia* sp. stimulate Th1 responses by engaging TLR2 and TLR4 (47). Similar endosymbionts have not been identified in the genus *Trichinella* and the stimulus for Th1 cells has not been investigated. We observed that the Th1 response is prominent only during acute infection, a time that is coincident with significant damage to host muscle cells caused by parasite migration and growth. It has been reported that tissue damage releases extracellular matrix proteins that can trigger activation of dendritic cells and macrophages. For example, heparan sulfate, a major component of extracellular matrix and cell membranes, stimulates TLR4-dependent maturation of dendritic cells resulting in production of proinflammatory cytokines TNF-α, IL-6, and IL-1β (48, 49). Skeletal muscle and *T. spiralis* nurse cells are rich in heparan sulfate (50). Leukocytes recruited to sites of infection may be exposed to cytoplasmic contents of muscle cells that stimulate production of proinflammatory cytokines. IL-10 may be produced to control such pathological responses to tissue damage.

Treg have been shown to require IL-10 to mediate protection from Th1-driven intestinal inflammation (10, 11); therefore, we investigated whether this cell population was important in control of Th1 responses and myositis during *T. spiralis* infection. Infection induced an enrichment of $CD4^+Foxp3^+$ Treg in the diaphragm. We found that reducing the proportion of Treg in the infected diaphragm by anti-CD25 treatment was associated with increased parasite-specific Th2 cytokine production but did not influence myositis. Because anti-CD25 treatment did not deplete all $Foxp3^+$ cells, it is possible that the residual Treg may have limited the inflammatory response in depleted mice; however, the contrasting responses in IL-$10^{-/-}$ and Treg-depleted mice suggest that the two modulators work independently.

We took a mechanistic approach to identifying cells that mediate IL-10-dependent suppression of inflammation. Focusing on CD4 T cell populations, we conducted adoptive transfer experiments with $CD4^+CD25^-$ and $CD4^+CD25^+$ cells derived from infected WT and IL-$10^{-/-}$ donors. Because recipient mice were RAG2$^{-/-}$/IL-$10^{-/-}$, the source of IL-10 was restricted to donor Treg and/or Teff. We found that IL-10 production by $CD4^+CD25^-$ cells was sufficient to control myositis and IFN-γ production. IL-10 production has been described in suppressive CD4 T cell populations that may cosecrete Th2 and/or Th1 cytokines (reviewed in Ref. 51). These cells typically do not express CD25, and it is possible they may contribute to the suppressive effects we observed with $CD4^+CD25^-$ cells. Regardless, our results clearly illustrate that the $CD4^+$ Th cell population must simultaneously balance effector function with control of inflammation during muscle infection, and that IL-10 production contributes to this control.

TGF-β and IL-10 have been shown to have an additive effect in the suppression of T cell activity in vitro (52) and to reduce the in vitro larvicidal activity of IFN-γ-activated macrophages against schistosomula (53), yet few studies have examined this cooperative relationship in vivo during infection. Neutralization of TGF-β in IL-$10^{-/-}$ mice infected with *T. spiralis* resulted in myositis that was more severe than that seen in mice deficient in IL-10 or TGF-β alone. More importantly, this treatment resulted in parasite killing. This constitutes the first demonstration of cooperation between TGF-β and IL-10 that promotes parasite survival while protecting host tissue. TGF-β is a pleiotropic cytokine and our data raise interesting questions about the nature of its effect on *T. spiralis* infection. TGF-β signaling regulates the development of free-living nematodes, and there is great interest in understanding whether parasitic nematodes might depend upon host cytokines for growth and development (54). We did not observe a significant effect on parasite survival when TGF-β was neutralized in WT mice; therefore, our data argue against a requirement for host TGF-β in development of *T. spiralis* in the muscle. Although IL-10 and TGF-β both limited myositis, the two had very different effects on the cytokine response during infection. TGF-β appeared to attenuate the predominant cytokine response whereas IL-10 specifically targeted the Th1 response.

To better understand the types of T cell responses associated with parasite killing, we primed and challenged WT and IL-$10^{-/-}$ mice with NBL. We found that in WT mice, the memory response to infection was Th2 polarized and was associated with only modest reduction in muscle larvae. These results were similar to those obtained in Treg-depleted mice, where an enhanced Th2 response occurred in the absence of parasite killing. In contrast, in challenged, IL-10-deficient mice, Th2 responses were maintained while IFN-γ was markedly increased, resulting in a mixed memory response that was associated with evidence of parasite killing. Similarly, enhanced Th1 responses in IL-10/TGF-β-deficient mice destroyed larvae during primary infection. In aggregate, our results show that poorly regulated Th1 responses can destroy larvae, whereas Th2 responses are largely not destructive. Our results differ from those obtained with *Brugia pahangi* (55) and *Litomosoides sigmodontis* (16), in which elevated Th2 responses after Treg depletion resulted in parasite clearance. In the case of *L. sigmodontis*, Treg depletion resulted in elimination of >70% of the parasite burden (16).

Tissue distribution and intracellular vs extracellular location of worms may influence the requirements for parasite destruction (56). Extracellular filarial nematodes are highly susceptible to eosinophil-mediated killing (57, 58), while there is limited and contradictory evidence that intracellular *T. spiralis* muscle larvae are vulnerable to attack by eosinophils (59–61). Several expressed sequence tag clusters encoding antioxidants were found in mature *T. spiralis* muscle larvae, but not in NBL (62), suggesting that immature larvae may be vulnerable to oxidative or nitrosative damage. Indeed, it has been reported that NBL are highly susceptible to oxidative killing (63). Evidence from in vitro studies has shown that TGF-β can impair NO generation in macrophages by reducing the stability and translation of iNOS mRNA and increasing degradation of iNOS protein (64). We hypothesize that IL-10 and TGF-β cooperate to limit oxidative and/or nitrosative damage to the developing muscle larva or the host muscle cell. The role of iNOS in parasite killing can be tested using specific inhibitors. It is important to note that parasite death in the muscle was not associated with significant host morbidity, allowing us to test our

hypothesis and examine potential killing mechanisms in otherwise healthy animals.

Collectively, our data support a model of T cell suppression during muscle infection whereby Teff-derived IL-10 limits acute myositis, IFN-γ levels, and local iNOS production. In the presence of IL-10, Th2 cytokines are produced and that production is regulated by $CD4^+Foxp3^+$ cells. TGF-β, produced by unknown cell types, helps balance the T cell response and limits inflammation. In combination, these modulatory influences protect parasites in the muscle and limit tissue damage.

Acknowledgments

We thank Dr. Daniel Rifkin for providing mink-lung epithelial cells and Dr. Edward Pearce for helpful suggestions.

Disclosures

The authors have no financial conflict of interest.

References

1. Bell, R. G., and C. H. Wang. 1987. The *Trichinella spiralis* newborn larvae: production, migration and immunity in vivo. *Wiad. Parazytol.* 33: 453–478.
2. Stewart, G. L., and L. M. Charniga. 1980. Distribution of *Trichinella spiralis* in muscles of the mouse. *J. Parasitol.* 66: 688–689.
3. Ritterson, A. L. 1966. Nature of the cyst of *Trichinella spiralis*. *J. Parasitol.* 52: 157–161.
4. Humes, A. G., and R. P. Akers. 1952. Vascular changes in the cheek pouch of the golden hamster during infection with *Trichinella spiralis* larvae. *Anat. Rec.* 114: 103–113.
5. Jasmer, D. P. 1993. *Trichinella spiralis* infected skeletal muscle cells arrest in G_2-M and cease muscle gene expression. *J. Cell Biol.* 121: 785–793.
6. Despommier, D. 1975. Adaptive changes in muscle fibers infected with *Trichinella spiralis*. *Am. J. Pathol.* 78: 477–496.
7. King, C. L., S. Mahanty, V. Kumaraswami, J. S. Abrams, J. Regunathan, K. Jayaraman, E. A. Ottesen, and T. B. Nutman. 1993. Cytokine control of parasite-specific anergy in human lymphatic filariasis: preferential induction of a regulatory T helper type 2 lymphocyte subset. *J. Clin. Invest.* 92: 1667–1673.
8. Babu, S., C. P. Blauvelt, V. Kumaraswami, and T. B. Nutman. 2006. Regulatory networks induced by live parasites impair both Th1 and Th2 pathways in patent lymphatic filariasis: implications for parasite persistence. *J. Immunol.* 176: 3248–3256.
9. Doetze, A., J. Satoguina, G. Burchard, T. Rau, C. Loliger, B. Fleischer, and A. Hoerauf. 2000. Antigen-specific cellular hyporesponsiveness in a chronic human helminth infection is mediated by T $3/T_r$ 1-type cytokines IL-10 and transforming growth factor-β but not by a T_h1 to T_h2 shift. *Int. Immunol.* 12: 623–630.
10. Asseman, C., S. Mauze, M. W. Leach, R. L. Coffman, and F. Powrie. 1999. An essential role for interleukin 10 in the function of regulatory T cells that inhibit intestinal inflammation. *J. Exp. Med.* 190: 995–1004.
11. Maloy, K. J., L. Salaun, R. Cahill, G. Dougan, N. J. Saunders, and F. Powrie. 2003. $CD4^+CD25^+$ T_R cells suppress innate immune pathology through cytokine-dependent mechanisms. *J. Exp. Med.* 197: 111–119.
12. Taylor, J. J., M. Mohrs, and E. J. Pearce. 2006. Regulatory T cell responses develop in parallel to Th responses and control the magnitude and phenotype of the Th effector population. *J. Immunol.* 176: 5839–5847.
13. Baumgart, M., F. Tompkins, J. Leng, and M. Hesse. 2006. Naturally occurring $CD4^+Foxp3^+$ regulatory T cells are an essential, IL-10-independent part of the immunoregulatory network in *Schistosoma mansoni* egg-induced inflammation. *J. Immunol.* 176: 5374–5387.
14. Hesse, M., C. A. Piccirillo, Y. Belkaid, J. Prufer, M. Mentink-Kane, M. Leusink, A. W. Cheever, E. M. Shevach, and T. A. Wynn. 2004. The pathogenesis of schistosomiasis is controlled by cooperating IL-10-producing innate effector and regulatory T cells. *J. Immunol.* 172: 3157–3166.
15. McKee, A. S., and E. J. Pearce. 2004. $CD25^+CD4^+$ cells contribute to Th2 polarization during helminth infection by suppressing Th1 response development. *J. Immunol.* 173: 1224–1231.
16. Taylor, M. D., L. LeGoff, A. Harris, E. Malone, J. E. Allen, and R. M. Maizels. 2005. Removal of regulatory T cell activity reverses hyporesponsiveness and leads to filarial parasite clearance in vivo. *J. Immunol.* 174: 4924–4933.
17. Finkelman, F. D., T. Shea-Donohue, S. C. Morris, L. Gildea, R. Strait, K. B. Madden, L. Schopf, and J. F. Urban, Jr. 2004. Interleukin-4- and interleukin-13-mediated host protection against intestinal nematode parasites. *Immunol. Rev.* 201: 139–155.
18. Fallon, P. G., H. E. Jolin, P. Smith, C. L. Emson, M. J. Townsend, R. Fallon, and A. N. McKenzie. 2002. IL-4 induces characteristic Th2 responses even in the combined absence of IL-5, IL-9, and IL-13. *Immunity* 17: 7–17.
19. Akiho, H., Y. Deng, P. Blennerhassett, H. Kanbayashi, and S. M. Collins. 2005. Mechanisms underlying the maintenance of muscle hypercontractility in a model of postinfective gut dysfunction. *Gastroenterology* 129: 131–141.
20. Urban, J. F., Jr., N. Noben-Trauth, D. D. Donaldson, K. B. Madden, S. C. Morris, M. Collins, and F. D. Finkelman. 1998. IL-13, IL-4Rα, and Stat6 are required for the expulsion of the gastrointestinal nematode parasite *Nippostrongylus brasiliensis*. *Immunity* 8: 255–264.
21. Urban, J. F., Jr., I. M. Katona, W. E. Paul, and F. D. Finkelman. 1991. Interleukin 4 is important in protective immunity to a gastrointestinal nematode infection in mice. *Proc. Natl. Acad. Sci. USA* 88: 5513–5517.
22. Else, K. J., F. D. Finkelman, C. R. Maliszewski, and R. K. Grencis. 1994. Cytokine-mediated regulation of chronic intestinal helminth infection. *J. Exp. Med.* 179: 347–351.
23. Schopf, L. R., K. F. Hoffmann, A. W. Cheever, J. F. Urban, Jr., and T. A. Wynn. 2002. IL-10 is critical for host resistance and survival during gastrointestinal helminth infection. *J. Immunol.* 168: 2383–2392.
24. Hoffmann, K. F., A. W. Cheever, and T. A. Wynn. 2000. IL-10 and the dangers of immune polarization: excessive type 1 and type 2 cytokine responses induce distinct forms of lethal immunopathology in murine schistosomiasis. *J. Immunol.* 164: 6406–6416.
25. Crum, E. D., D. D. Despommier, and D. D. McGregor. 1977. Immunity to *Trichinella spiralis* I: transfer of resistance by two classes of lymphocytes. *Immunology* 33: 787–795.
26. Beiting, D. P., S. K. Bliss, D. H. Schlafer, V. L. Roberts, and J. A. Appleton. 2004. Interleukin-10 limits local and body cavity inflammation during infection with muscle-stage *Trichinella spiralis*. *Infect. Immun.* 72: 3129–3137.
27. Appleton, J. A., and L. Usack. 1993. Identification of potential antigenic targets for rapid expulsion of *Trichinella spiralis*. *Mol. Biochem. Parasitol.* 58: 53–62.
28. Lowenthal, J. W., P. Corthesy, C. Tougne, R. Lees, H. R. MacDonald, and M. Nabholz. 1985. High and low affinity IL 2 receptors: analysis by IL 2 dissociation rate and reactivity with monoclonal anti-receptor antibody PC61. *J. Immunol.* 135: 3988–3994.
29. Dasch, J. R., D. R. Pace, W. Waegell, D. Inenaga, and L. Ellingsworth. 1989. Monoclonal antibodies recognizing transforming growth factor-β: bioactivity neutralization and transforming growth factor β2 affinity purification. *J. Immunol.* 142: 1536–1541.
30. Appleton, J. A., D. F. Antczak, and A. D. Lopes. 1987. Characterization of the equine influenza virus H3 with monoclonal antibodies. *Arch. Virol.* 94: 339–346.
31. Daley, L. P., L. F. Gagliardo, M. S. Duffy, M. C. Smith, and J. A. Appleton. 2005. Application of monoclonal antibodies in functional and comparative investigations of heavy-chain immunoglobulins in new world camelids. *Clin. Diagn. Lab. Immunol.* 12: 380–386.
32. Bliss, S. K., A. Alcaraz, and J. A. Appleton. 2003. IL-10 prevents liver necrosis during murine infection with *Trichinella spiralis*. *J. Immunol.* 171: 3142–3147.
33. Kaplan, M. H., U. Schindler, S. T. Smiley, and M. J. Grusby. 1996. Stat6 is required for mediating responses to IL-4 and for development of Th2 cells. *Immunity* 4: 313–319.
34. Kohm, A. P., J. S. McMahon, J. R. Podojil, W. S. Begolka, M. Degutes, D. J. Kasprowicz, S. F. Ziegler, and S. D. Miller. 2006. Cutting edge: anti-CD25 monoclonal antibody injection results in the functional inactivation, not depletion, of $CD4^+CD25^+$ T regulatory cells. *J. Immunol.* 176: 3301–3305.
35. Konaka, Y., M. A. Norcross, V. C. Maino, and R. T. Smith. 1981. Anti-Thy-1-mediated T cell activation: role of soluble factors and expression of interleukin 2 receptors on T cells. *Eur. J. Immunol.* 11: 445–450.
36. Kroczek, R. A., C. D. Black, J. Barbet, L. J. Edison, and E. M. Shevach. 1987. Induction of IL-2 receptor expression in vivo: response to allogeneic cells. *Transplantation* 44: 547–553.
37. Sakaguchi, S., N. Sakaguchi, M. Asano, M. Itoh, and M. Toda. 1995. Immunologic self-tolerance maintained by activated T cells expressing IL-2 receptor α-chains (CD25): breakdown of a single mechanism of self-tolerance causes various autoimmune diseases. *J. Immunol.* 155: 1151–1164.
38. Kitani, A., I. Fuss, K. Nakamura, F. Kumaki, T. Usui, and W. Strober. 2003. Transforming growth factor (TGF)-β1-producing regulatory T cells induce Smad-mediated interleukin 10 secretion that facilitates coordinated immunoregulatory activity and amelioration of TGF-β1-mediated fibrosis. *J. Exp. Med.* 198: 1179–1188.
39. Nakamura, K., A. Kitani, I. Fuss, A. Pedersen, N. Harada, H. Nawata, and W. Strober. 2004. TGF-β 1 plays an important role in the mechanism of $CD4^+CD25^+$ regulatory T cell activity in both humans and mice. *J. Immunol.* 172: 834–842.
40. Nakamura, K., A. Kitani, and W. Strober. 2001. Cell contact-dependent immunosuppression by $CD4^+CD25^+$ regulatory T cells is mediated by cell surface-bound transforming growth factor β. *J. Exp. Med.* 194: 629–644.
41. Abe, M., J. G. Harpel, C. N. Metz, I. Nunes, D. J. Loskutoff, and D. B. Rifkin. 1994. An assay for transforming growth factor-β using cells transfected with a plasminogen activator inhibitor-1 promoter-luciferase construct. *Anal. Biochem.* 216: 276–284.
42. Sadler, C. H., L. I. Rutitzky, M. J. Stadecker, and R. A. Wilson. 2003. IL-10 is crucial for the transition from acute to chronic disease state during infection of mice with *Schistosoma mansoni*. *Eur. J. Immunol.* 33: 880–888.
43. Wynn, T. A., R. Morawetz, T. Scharton-Kersten, S. Hieny, H. C. Morse, III, R. Kuhn, W. Muller, A. W. Cheever, and A. Sher. 1997. Analysis of granuloma formation in double cytokine-deficient mice reveals a central role for IL-10 in polarizing both T helper cell 1- and T helper cell 2-type cytokine responses in vivo. *J. Immunol.* 159: 5014–5023.
44. Kullberg, M. C., J. M. Ward, P. L. Gorelick, P. Caspar, S. Hieny, A. Cheever, D. Jankovic, and A. Sher. 1998. *Helicobacter hepaticus* triggers colitis in specific-pathogen-free interleukin-10 (IL-10)-deficient mice through an IL-12- and γ interferon-dependent mechanism. *Infect. Immun.* 66: 5157–5166.
45. Kullberg, M. C., A. G. Rothfuchs, D. Jankovic, P. Caspar, T. A. Wynn, P. L. Gorelick, A. W. Cheever, and A. Sher. 2001. *Helicobacter hepaticus*-induced colitis in interleukin-10-deficient mice: cytokine requirements for the induction and maintenance of intestinal inflammation. *Infect. Immun.* 69: 4232–4241.

46. Osborne, J., and E. Devaney. 1999. Interleukin-10 and antigen-presenting cells actively suppress Th1 cells in BALB/c mice infected with the filarial parasite *Brugia pahangi*. *Infect. Immun.* 67: 1599–1605.
47. Brattig, N. W., C. Bazzocchi, C. J. Kirschning, N. Reiling, D. W. Buttner, F. Ceciliani, F. Geisinger, H. Hochrein, M. Ernst, H. Wagner, et al. 2004. The major surface protein of *Wolbachia endosymbionts* in filarial nematodes elicits immune responses through TLR2 and TLR4. *J. Immunol.* 173: 437–445.
48. Johnson, G. B., G. J. Brunn, Y. Kodaira, and J. L. Platt. 2002. Receptor-mediated monitoring of tissue well-being via detection of soluble heparan sulfate by Toll-like receptor 4. *J. Immunol.* 168: 5233–5239.
49. Kodaira, Y., S. K. Nair, L. E. Wrenshall, E. Gilboa, and J. L. Platt. 2000. Phenotypic and functional maturation of dendritic cells mediated by heparan sulfate. *J. Immunol.* 165: 1599–1604.
50. Beiting, D. P., P. W. Park, and J. A. Appleton. 2006. Synthesis of syndecan-1 by skeletal muscle cells is an early response to infection with *Trichinella spiralis* but is not essential for nurse cell development. *Infect. Immun.* 74: 1941–1943.
51. Hawrylowicz, C. M., and A. O'Garra. 2005. Potential role of interleukin-10-secreting regulatory T cells in allergy and asthma. *Nat. Rev. Immunol.* 5: 271–283.
52. Zeller, J. C., A. Panoskaltsis-Mortari, W. J. Murphy, F. W. Ruscetti, S. Narula, M. G. Roncarolo, and B. R. Blazar. 1999. Induction of $CD4^+$ T cell alloantigen-specific hyporesponsiveness by IL-10 and TGF-β. *J. Immunol.* 163: 3684–3691.
53. Oswald, I. P., R. T. Gazzinelli, A. Sher, and S. L. James. 1992. IL-10 synergizes with IL-4 and transforming growth factor-β to inhibit macrophage cytotoxic activity. *J. Immunol.* 148: 3578–3582.
54. Viney, M. E., F. J. Thompson, and M. Crook. 2005. TGF-β and the evolution of nematode parasitism. *Int. J. Parasitol.* 35: 1473–1475.
55. Gillan, V., and E. Devaney. 2005. Regulatory T cells modulate Th2 responses induced by *Brugia pahangi* third-stage larvae. *Infect. Immun.* 73: 4034–4042.
56. Mulcahy, G., S. O'Neill, J. Fanning, E. McCarthy, and M. Sekiya. 2005. Tissue migration by parasitic helminths—an immunoevasive strategy? *Trends Parasitol.* 21: 273–277.
57. Martin, C., L. Le Goff, M. N. Ungeheuer, P. N. Vuong, and O. Bain. 2000. Drastic reduction of a filarial infection in eosinophilic interleukin-5 transgenic mice. *Infect. Immun.* 68: 3651–3656.
58. Volkmann, L., O. Bain, M. Saeftel, S. Specht, K. Fischer, F. Brombacher, K. I. Matthaei, and A. Hoerauf. 2003. *Murine filariasis*: interleukin 4 and interleukin 5 lead to containment of different worm developmental stages. *Med. Microbiol. Immunol.* 192: 23–31.
59. Gurish, M. F., A. Humbles, H. Tao, S. Finkelstein, J. A. Boyce, C. Gerard, D. S. Friend, and K. F. Austen. 2002. CCR3 is required for tissue eosinophilia and larval cytotoxicity after infection with *Trichinella spiralis*. *J. Immunol.* 168: 5730–5736.
60. Herndon, F. J., and S. G. Kayes. 1992. Depletion of eosinophils by anti-IL-5 monoclonal antibody treatment of mice infected with *Trichinella spiralis* does not alter parasite burden or immunologic resistance to reinfection. *J. Immunol.* 149: 3642–3647.
61. Hokibara, S., M. Takamoto, A. Tominaga, K. Takatsu, and K. Sugane. 1997. Marked eosinophilia in interleukin-5 transgenic mice fails to prevent *Trichinella spiralis* infection. *J. Parasitol.* 83: 1186–1189.
62. Mitreva, M., D. P. Jasmer, J. Appleton, J. Martin, M. Dante, T. Wylie, S. W. Clifton, R. H. Waterston, and J. P. McCarter. 2004. Gene discovery in the adenophorean nematode *Trichinella spiralis*: an analysis of transcription from three life cycle stages. *Mol. Biochem. Parasitol.* 137: 277–291.
63. Kazura, J. W., and S. R. Meshnick. 1984. Scavenger enzymes and resistance to oxygen mediated damage in *Trichinella spiralis*. *Mol. Biochem. Parasitol.* 10: 1–10.
64. Vodovotz, Y., C. Bogdan, J. Paik, Q. W. Xie, and C. Nathan. 1993. Mechanisms of suppression of macrophage nitric oxide release by transforming growth factor β. *J. Exp. Med.* 178: 605–613.